Anomalous spatio-temporal chaos in a two-dimensional system of nonlocally coupled oscillators

Nakao, H

CHAOS VOLUME 9, NUMBER 4 DECEMBER 1999

Anomalous spatio-temporal chaos in a two-dimensional system of nonlocally coupled oscillators

Hiroya Nakao[a)]
Department of Physics, Graduate School of Sciences, Kyoto University, Kyoto 606-8502, Japan

(Received 19 March 1999; accepted for publication 13 August 1999)

A two-dimensional system of nonlocally coupled complex Ginzburg–Landau oscillators is investigated numerically for the first time. As previously shown for the one-dimensional case, this two-dimensional system exhibits anomalous spatio-temporal chaos characterized by power-law spatial correlations. In this chaotic regime, the amplitude difference between neighboring elements displays temporal noisy on–off intermittency. The system is also spatially intermittent in this regime, as revealed by multiscaling analysis: The amplitude field is multiaffine and the difference field is multifractal. Correspondingly, the probability distribution function of the measure defined for each field is strongly non-Gaussian, exhibiting scale-dependent deviations in the tail due to intermittency. © *1999 American Institute of Physics.* [S1054-1500(99)01304-X]

Assemblies of mutually interacting dynamical units are ubiquitous in nature. As models for them, systems of simple coupled dynamical elements, e.g., limit cycle oscillators and chaotic maps, have been studied extensively. Recently, a new class of coupled systems, those with nonlocally coupled dynamical elements, was introduced and found to exhibit anomalous spatio-temporal chaos characterized by power-law spatial correlations. All previous studies on such systems have been done in one dimension, but the mechanism for the appearance of this spatio-temporal chaos seems to be universal, and it is also expected to exist in higher dimensions. In this paper, a two-dimensional system of nonlocally coupled oscillators is investigated for the first time. As in the one-dimensional case, the system is found to exhibit anomalous spatio-temporal chaos, accompanied by several distinctive features specific to this chaotic regime: Power-law spatial correlations, noisy on–off intermittency, and multiscaling properties.

I. INTRODUCTION

Assemblies of coupled dynamical elements are widely observed in nature. Simplified models of such systems, e.g., coupled limit cycle oscillators and chaotic maps, have played important roles not only in modeling such systems realistically but also in understanding the varieties of possible behavior of systems far from equilibrium. Many important concepts, such as pattern formation and spatio-temporal chaos, have been extracted from detailed studies of such models.

The interaction between elements is usually assumed to be attractive, and of a mean-field type in a wide sense; each element is coupled to the mean amplitude of its neighboring elements, and is driven by the difference between its own amplitude and this mean amplitude in such a way that the amplitude differences between elements tend to decrease.

A system with diffusive coupling is a representative limiting case. Here, each element interacts strongly with its nearest neighbors, so that the amplitude field of the system is always continuous and smooth. It is well known that some equations describing diffusively coupled systems of dynamical elements, such as the complex Ginzburg–Landau equation, exhibit spatio-temporal chaos.[1,2]

The opposite limiting case is that of global coupling, or mean-field coupling in the narrow sense. Here, each element is coupled to the mean field of the entire system, and is thus coupled to all elements with equal strength. In this case, the amplitude field becomes statistically spatially homogeneous, and the notion of space is lost. It is known that systems with global coupling generally exhibit some typical forms of behavior, e.g., clustering and collective chaos.[3,4]

In Ref. 5, Kuramoto introduced a system lying between the above two limiting cases, one of nonlocally coupled elements. Our subsequent numerical simulations of one-dimensional, nonlocally coupled systems with various types of elements revealed that such systems generally exhibit anomalous spatio-temporal chaotic behavior, which cannot be seen in the two limiting cases. In this chaotic regime, the amplitude field becomes fractal, and the spatial correlation of the amplitude field displays power-law behavior on small scales. Furthermore, the fractal dimension and the exponent of the spatial correlation vary continuously with the coupling strength. We developed a theory, based on a simple multiplicative stochastic model,[6,7] that can explain the fractality of the amplitude field and the power-law behavior of the spatial correlation. Such a model is frequently employed in describing the noisy on–off intermittency phenomena[8–10] found in many physical systems, and this suggests that our system too likely exhibits this type of temporal intermittency. The temporal intermittency of our system induces a spatial intermittency. In order to study this, we carried out a more general analysis of the amplitude field based on qth structure functions and found that the amplitude field possesses multiaffin-

[a)]Present address: Graduate School of Mathematical Sciences, University of Tokyo, 3-8-1 Komaba, Meguro, Tokyo 153-8914, Japan. Electronic mail: nakao@ton.scphys.kyoto-u.ac.jp

ity. We also carried out multifractal analysis of the difference field of the original amplitude field, inspired by its apparent similarity to the intermittent energy dissipation field in fluid turbulence.[6,11]

All our previous studies were done in one-dimensional systems. However, our previous theory does not require the systems to be one-dimensional, and spatio-temporal chaos with power-law structure functions is also expected in higher dimensions. In this paper, we study a system of nonlocally coupled complex Ginzburg–Landau oscillators in two dimensions for the first time, and investigate the anomalous spatio-temporal chaotic regime of this system. Some consideration is given to the multiscaling properties of the intermittent amplitude and difference fields.

II. MODEL

As proposed by Kuramoto,[5] nonlocal coupling naturally appears in the following plausible situation. Consider an assembly of spatially distributed dynamical elements, e.g., cells. Each element is assumed to interact indirectly with other elements through some (e.g., chemical) substance, which diffuses and decays much faster than the dynamics of each element. Such a situation can be described by the set of equations

$$\dot{\boldsymbol{X}}(\boldsymbol{r},t)=\boldsymbol{F}(\boldsymbol{X}(\boldsymbol{r},t))+\mathbf{K}\cdot\boldsymbol{A}(\boldsymbol{r},t), \tag{1}$$

$$\epsilon\dot{\boldsymbol{A}}(\boldsymbol{r},t)=-\eta\boldsymbol{A}(\boldsymbol{r},t)+D\nabla^2\boldsymbol{A}(\boldsymbol{r},t)+\boldsymbol{X}(\boldsymbol{r},t), \tag{2}$$

where $\boldsymbol{X}$ is the amplitude of an element, $\boldsymbol{F}$ describes the intrinsic dynamics of the amplitude in the absence of coupling, and $\boldsymbol{A}$ is the concentration of the intermediating substance with decay rate η and diffusion rate D. The substance $\boldsymbol{A}$ is generated at a rate proportional to the amplitude $\boldsymbol{X}$, and the amplitude $\boldsymbol{X}$ is affected by the substance $\boldsymbol{A}$ through a coupling matrix $\mathbf{K}$. The parameter ϵ determines the ratio of the time scale of the elements to that of the substance, and is assumed to be very small.

Now, let us consider the $\epsilon\to 0$ limit and eliminate the dynamics of $\boldsymbol{A}$ adiabatically. Setting the left-hand side of Eq. (2) to 0, we can solve the equation for $\boldsymbol{A}$ as

$$\boldsymbol{A}(\boldsymbol{r},t)=\int d\boldsymbol{r}'\,G(\boldsymbol{r}'-\boldsymbol{r})\boldsymbol{X}(\boldsymbol{r}',t), \tag{3}$$

where $G(\boldsymbol{r}'-\boldsymbol{r})$ is a kernel that satisfies

$$(\eta-D\nabla^2)G(\boldsymbol{r}'-\boldsymbol{r})=\delta(\boldsymbol{r}'). \tag{4}$$

By inserting Eq. (3) into Eq. (1), we obtain the following system of nonlocally coupled dynamical elements

$$\dot{\boldsymbol{X}}(\boldsymbol{r},t)=\boldsymbol{F}(\boldsymbol{X}(\boldsymbol{r},t))+\mathbf{K}\cdot\int d\boldsymbol{r}'\,G(\boldsymbol{r}'-\boldsymbol{r})\boldsymbol{X}(\boldsymbol{r}',t). \tag{5}$$

The kernel $G(\boldsymbol{r}'-\boldsymbol{r})$ can be solved as

$$G(\boldsymbol{r}'-\boldsymbol{r})=\frac{1}{(2\pi)^d}\int d^d\boldsymbol{q}\frac{\exp[i\boldsymbol{q}\cdot(\boldsymbol{r}'-\boldsymbol{r})]}{\eta+D|\boldsymbol{q}|^2}, \tag{6}$$

where d is the spatial dimension of the system. When the system is isotropic, the kernel G becomes a function of the distance $r:=|\boldsymbol{r}'-\boldsymbol{r}|$, and can be expressed as

$$G(r)\propto\exp(-\gamma|r|),\quad d=1, \tag{7}$$

$$K_0(\gamma|r|),\quad d=2, \tag{8}$$

$$\frac{\exp(-\gamma|r|)}{\gamma|r|},\quad d=3, \tag{9}$$

where K_0 is the modified Bessel function. The constant γ is the inverse of the coupling length and is given by

$$\gamma=\sqrt{\frac{\eta}{D}}. \tag{10}$$

Each $G(r)$ must satisfy the normalization condition $\int G(r)d^d\boldsymbol{r}=1$. Since we treat a two-dimensional system, we use Eq. (8) for $G(r)$ hereafter.

As elements, we use complex Ginzburg–Landau oscillators. They are the simplest limit cycle oscillators that can be derived through the center-manifold reduction technique from generic oscillators near their Hopf bifurcation points.[1] The corresponding nonlocally coupled system is given by the following equation for the complex amplitude W (Here we explicitly include the term $-W$ in the coupling part in order to express that the coupling is actually attractive. It could as well be absorbed into the intrinsic part by rescaling the variables suitably.):

$$\dot{W}(\boldsymbol{r},t)=W-(1+ic_2)|W|^2W+K(1+ic_1)(\overline{W}-W). \tag{11}$$

Here K is the coupling strength, c_1 and c_2 are real parameters, and the nonlocal mean-field $\overline{W}$ is given by

$$\overline{W}(\boldsymbol{r},t)=\int d\boldsymbol{r}'\,G(\boldsymbol{r}'-\boldsymbol{r})W(\boldsymbol{r}',t). \tag{12}$$

This is the nonlocal complex Ginzburg–Landau equation introduced by Kuramoto[5] as the first concrete example of nonlocally coupled systems.

III. ANOMALOUS SPATIO-TEMPORAL CHAOS

In the numerical simulations whose results are presented here, the system was a square lattice of length 1. A total of $N^2=512^2-2048^2$ elements were situated at lattice sites, and periodic boundary conditions were used. The coupling length γ^{-1} was fixed to 1/8. The nonlocal mean field is easily calculated by using the FFT (fast Fourier transform) technique, since it is simply a convolution of the amplitude field with the kernel Eq. (8). We set $c_1=-2$ and $c_2=2$. These are the standard values used in our one-dimensional simulations.

In Figs. 1–3, typical snapshots of the real part $X(x,y)$ of the complex variable $W(x,y)$ are shown for three different values of the coupling strength K. (Since by symmetry we obtain similar figures for the imaginary part $Y(x,y)$, we use $X(x,y)$ in the following analysis and call it the ''amplitude field.'') The amplitude field at $K=1.05$ is continuous and smooth, while at $K=0.65$ it seems to be discontinuous and disordered, although not completely random. The amplitude field at the intermediate coupling strength $K=0.85$ looks somewhat more complex and intriguing; it is composed of

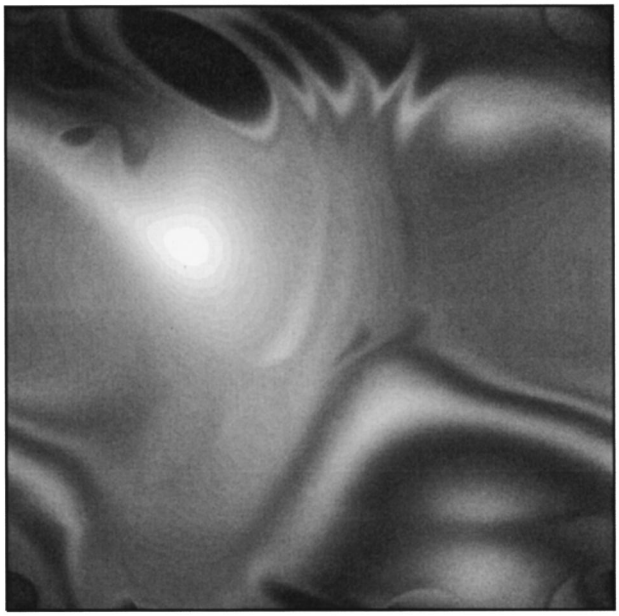

FIG. 1. Snapshot of the amplitude field $X(x,y)$ for $K=1.05$. Darker dots indicate larger amplitudes.

FIG. 3. Snapshot of the amplitude field $X(x,y)$ for $K=0.65$.

intricately convoluted, smooth and disordered patches of various length scales. This is the anomalous spatio-temporal chaotic regime in which we are interested.

IV. SPATIAL CORRELATION FUNCTION

Let us first examine the spatial correlation function. Figures 4(a)–4(c) display the spatial correlation functions $C(x,y):=\langle X(0,0)X(x,y)\rangle$ corresponding to the amplitude fields shown in Figs. 1–3. Each correlation function is clearly rotationally symmetric, resulting from the isotropy of the system. As the amplitude field becomes disordered, the correlation function becomes steep, and the center of the graph, which corresponds to the self-correlation $C(0,0)$, becomes peaked.

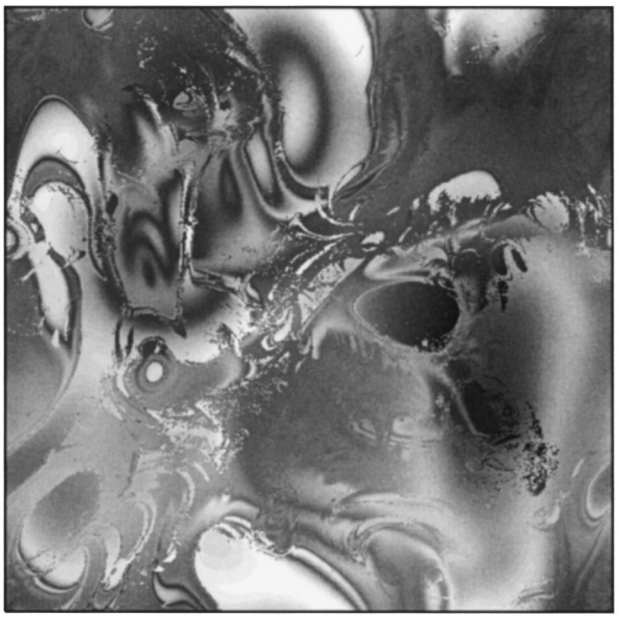

FIG. 2. Snapshot of the amplitude field $X(x,y)$ for $K=0.85$.

In Ref. 5, the anomalous spatio-temporal chaotic regime is characterized by the power-law behavior of the spatial correlation function at small distance:

$$C(l):=\langle X(0)X(l)\rangle \simeq C_0 - C_1 l^{\alpha} (l \ll 1), \tag{13}$$

where C_0 and C_1 are constants and α is a noninteger parameter-dependent exponent.

To confirm that this power-law behavior also exists in two dimensions. we calculated the radial correlation function $C(l)=\langle X(\boldsymbol{r})X(\boldsymbol{r}+\boldsymbol{l})\rangle$ $(|\boldsymbol{l}|=l)$ along a straight line in a certain direction [We mainly used the (0,1) and (1,1) directions, but the results are independent of the direction.], and fit for the best values of C_0 and C_1. Figure 5 displays $\ln l$ vs $\ln[C_0-C(l)]$ for several values of the coupling strength K. For each coupling strength, the experimental data fall almost along a single line, and the power-law behavior is evident. The exponent α of the power law varies continuously with the coupling strength. Although not shown in the figure, the correlation function $C(l)$ is continuous at the origin $l=0$ for $K \geqslant K_c$ and discontinuous for $K<K_c$, where $0.80<K_c<0.85$. At this value, there appears a finite gap between the self-correlation $C(0)$ and the correlation between the nearest-neighbor elements $\lim_{l\to+0} C(l) \simeq C_0$. This implies that the motion of each individual element becomes so violent that the amplitude field is no longer continuous statistically. In Ref. 7, this transition point is identified with the blowout bifurcation point in the on–off intermittent dynamics of the amplitude difference between nearby elements.

Thus, the anomalous spatio-temporal chaos in two dimensions is also characterized by power-law behavior of the spatial correlation function with a parameter-dependent exponent.

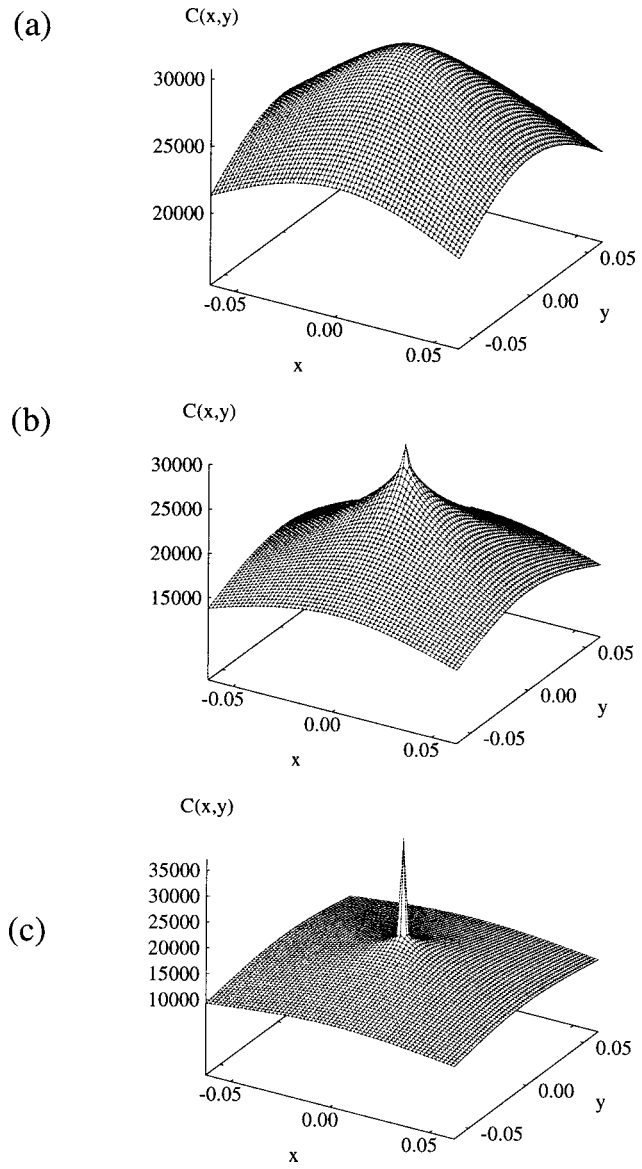

FIG. 4. Short-range spatial correlation functions $C(x,y)$ for (a) $K=1.05$, (b) $K=0.85$, and (c) $K=0.65$.

V. NOISY ON–OFF INTERMITTENCY

In Refs. 6 and 7, we argue that the scaling behavior of the spatial correlation is a consequence of the underlying multiplicative processes of amplitude differences between neighboring elements. We described this process using a multiplicative stochastic model and related the exponent α of the spatial correlation with the fluctuation of the finite-time Lyapunov exponent of an element. This model shares all essential features with those used in describing noisy on–off intermittency.[8–10] This suggests that our system should also exhibit this type of temporal intermittency. Actually, the finite-time Lyapunov exponent of an externally driven complex Ginzburg–Landau oscillator can fluctuate between positive and negative values, and neighboring oscillators are subjected to only slightly different nonlocal mean field. Therefore, the conditions for the appearance of noisy on–off intermittency between neighboring oscillators are satisfied in our system.

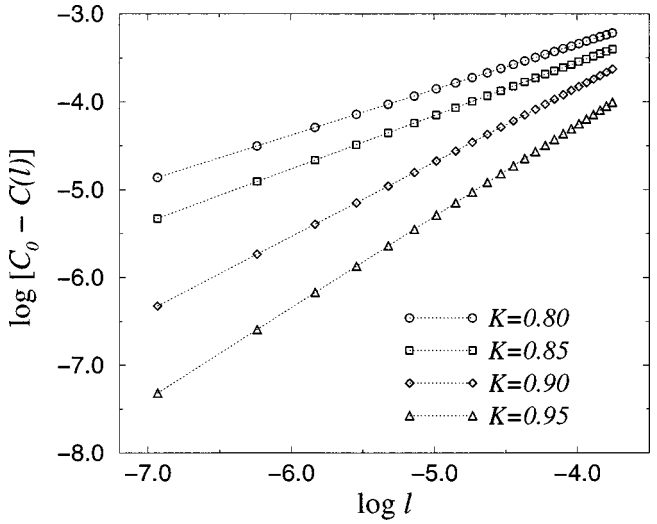

FIG. 5. Power-law behavior of the correlation functions: log–log plot of $C_0-C(l)$ vs l obtained for several values of the coupling strength K.

We now report results that confirm this for our system. The coupling strength K was set at 0.85. Figure 6 shows typical time sequences of the amplitude differences $\Delta X_1(t)$ and $\Delta X_2(t)$. The distance between the elements is 512^{-1} for $\Delta X_1(t)$ and 64^{-1} for $\Delta X_2(t)$. Strong intermittency of the signals is apparent. It can be seen that $\Delta X_2(t)$ exhibits more frequent bursts than $\Delta X_1(t)$, reflecting the fact that $\Delta X_2(t)$ is subjected to larger fluctuations than $\Delta X_1(t)$.

We can confirm that these intermittent signals actually represent noisy on–off intermittency by calculating the laminar length distribution. The laminar phase is defined as a continuous duration, during which the absolute value of the difference does not exceed a certain threshold. Here we choose 0.5 as the threshold value. Figure 7 displays laminar length distributions $R(t)$ obtained from $\Delta X_1(t)$ and $\Delta X_2(t)$. The characteristic shape of the distribution $R(t)$, i.e., the power-law dependence on t with slope $-3/2$ for small t together with the exponential shoulder seen in the large t region, clearly indicates that the signals actually correspond to

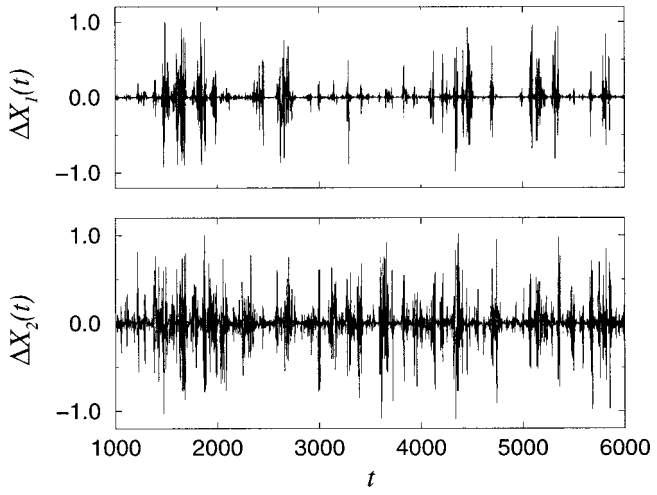

FIG. 6. Typical evolution of the amplitude differences. The distance between the elements is 512^{-1} for $\Delta X_1(t)$ and 64^{-1} for $\Delta X_2(t)$.

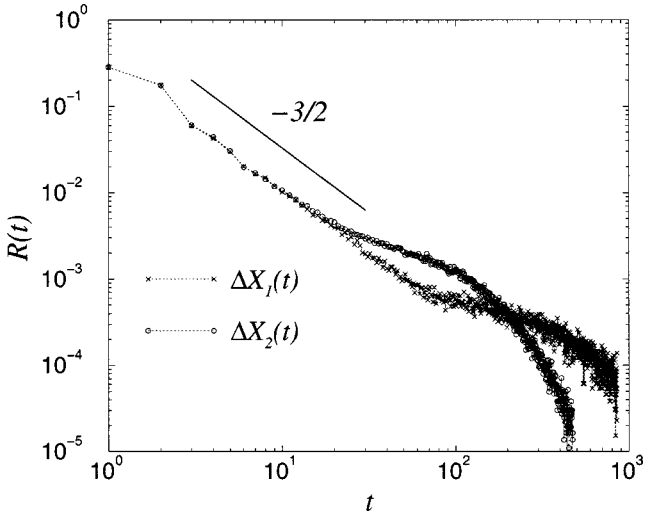

FIG. 7. Distributions of the laminar length obtained from the time sequences $\Delta X_1(t)$ and $\Delta X_2(t)$ shown in Fig. 6.

noisy on–off intermittency. The shoulder reflects broken scale invariance due to the additive noise. As expected, the shoulder of $\Delta X_2(t)$ appears at a smaller value of t than that of $\Delta X_1(t)$.[9,10]

VI. MULTISCALING ANALYSIS

The notion of multiscaling (i.e., multiaffinity and multifractality) has been employed successfully in characterizing complex spatio-temporal behavior of various phenomena, such as velocity and energy dissipation fields in fluid turbulence,[2,12] rough interfaces in fractal surface growth,[13] nematic fluid electro-convective turbulence,[14] financial data of currency exchange rates,[15] and even in natural images.[16] In Refs. 6 and 11, we introduced multiscaling analysis into our system for the one-dimensional case, inspired by the apparent similarity of the amplitude and difference fields in our system to the velocity and energy dissipation fields in fluid turbulence. Here we apply multiscaling analysis to the two-dimensional case.

First, we introduce the difference field $Z(\boldsymbol{r})$ as

$$Z(\boldsymbol{r}) := |\nabla X(\boldsymbol{r})| = \sqrt{\left(\frac{\partial X}{\partial x}\right)^2 + \left(\frac{\partial X}{\partial y}\right)^2}. \tag{14}$$

This quantity emphasizes the edges of the original amplitude field $X(\boldsymbol{r})$ (Here, the differential should not be interpreted literally. We always use a finite difference in the actual calculation, e.g., $[X(x+\Delta x,y)-X(x,y)]/\Delta x$ with sufficiently small Δx.). It is the analogue of the energy dissipation field in fluid turbulence. Figure 8 presents a typical snapshot of the difference field $Z(x,y)$ at $K=0.85$, corresponding to the amplitude field shown in Fig. 2. The intermittency underlying the original amplitude field is now apparent.

We then introduce the following quantities as measures for the amplitude field $X(\boldsymbol{r})$ and the difference field $Z(\boldsymbol{r})$:

$$h(\boldsymbol{r};l) := |X(\boldsymbol{r}+\boldsymbol{l}) - X(\boldsymbol{r})|, \tag{15}$$

$$m(\boldsymbol{r};l) := \int_{S(\boldsymbol{r};l)} Z(\boldsymbol{r}')\, d^2\boldsymbol{r}'. \tag{16}$$

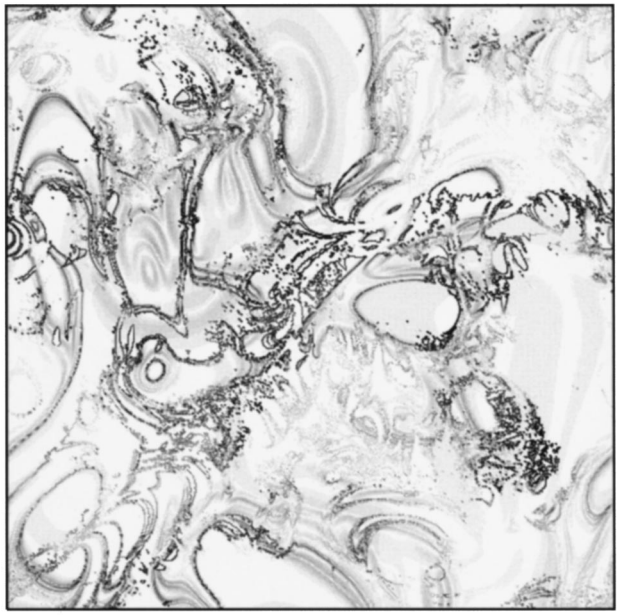

FIG. 8. Snapshot of the difference field $Z(x,y)$ for $K=0.85$, corresponding to the amplitude field shown in Fig. 2.

Here $|\boldsymbol{l}|=l$, and the domain of integration $S(\boldsymbol{r};l)$ is a square of length l placed at $\boldsymbol{r}$. The first quantity is the difference in the amplitude field $X(\boldsymbol{r})$ at two points separated by a distance l, and the second quantity is the volume enclosed by the difference field $Z(\boldsymbol{r})$ and the square $S(\boldsymbol{r};l)$.

Following the multifractal formalism, two types of partition functions are defined as

$$Z_h^q(l) := \langle h(l)^q \rangle = \frac{1}{M(l)} \sum_{i=1}^{M(l)} h(\boldsymbol{r}_i;l)^q, \tag{17}$$

$$Z_m^q(l) := N(l) \langle m(l)^q \rangle = \sum_{i=1}^{N(l)} m(\boldsymbol{r}_i;l)^q, \tag{18}$$

where $Z_h^q(l)$ is calculated along a certain line in some direction, as in the case of the previously considered spatial correlation function, while $Z_m^q(l)$ is calculated over the entire system. $\boldsymbol{r}_i$ is either the position of the line segment or the position of the square. $M(l)$ is the number of line segments of length l that are needed to cover the entire line, and $N(l)$ is the number of squares of size l that are needed to cover the entire system. The function $Z_h^q(l)$ is called the ''structure function'' in the context of fluid turbulence.[2,12]

When the measures possess scaling properties, the partition functions are expected to scale with l as $Z_h^q(l) \sim l^{\zeta(q)}$ and $Z_m^q(l) \sim l^{\tau(q)}$. Furthermore, if these exponents $\zeta(q)$ and $\tau(q)$ depend nonlinearly on q, the corresponding measures $h(l)$ and $m(l)$ are called ''multiaffine'' and ''multifractal,'' respectively.[2,12,13]

For the one-dimensional case, we know that the amplitude field is multiaffine and the difference field is multifractal. Moreover, our previous theory predicts the following form for the scaling exponent $\zeta(q)$ of the amplitude field:

$$\zeta(q) = q \ (0<q<\beta), \quad \beta \ (\beta<q). \tag{19}$$

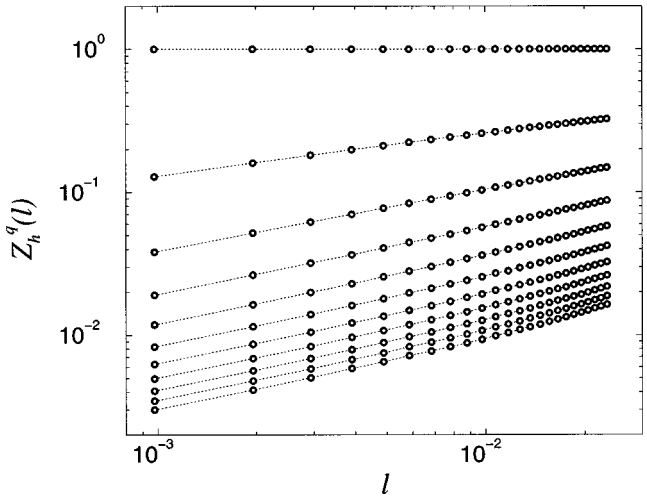

FIG. 9. Partition functions $Z_h^q(l)$ for several values of q, at intervals of 0.5. The top line corresponds to $q=0$, and the bottom one to $q=5$.

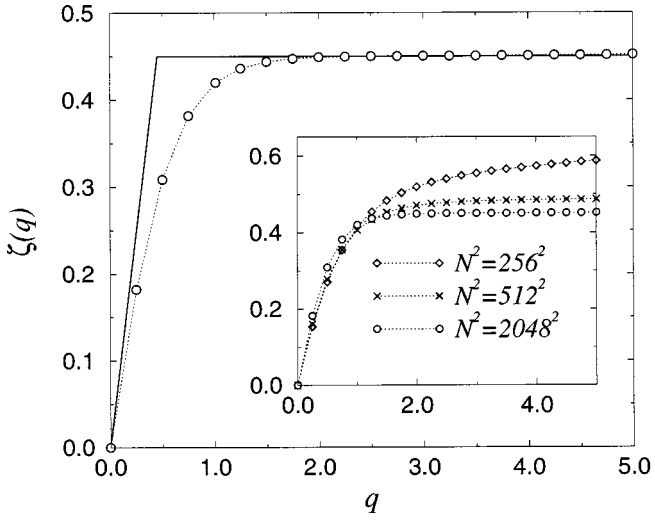

FIG. 10. Scaling exponent $\zeta(q)$ obtained for $N^2=2048^2$. The theoretical curve Eq. (19) with $\beta=0.45$ is compared with the experimental data. The dependence of the exponent spectra on the number of oscillators is shown in the inset for the cases $N^2=256^2$, 512^2, and 2048^2.

Here β is a positive constant determined by the fluctuation of the finite-time Lyapunov exponent of the element. It is related to the slope of the probability distribution of $h(l)$.[6,11] This is the simplest form of multiaffinity, and is sometimes referred to as ''bi-fractality.'' (There is some confusion in terminology for historical reasons. The term bi-affinity would be more appropriate.)[12] This form of the scaling exponent $\zeta(q)$ is also expected in two dimensions, since our previous theory imposes no restriction on the dimensionality of the system.

For the scaling exponent $\tau(q)$ of the difference field, we have not yet been able to develop a satisfactory theory. Numerical results in one-dimensional systems suggest that $\tau(q)$ also depends nonlinearly on q and that the difference field is multifractal with a rather simple functional form for $\tau(q)$.[11] However, the scaling exponent $\tau(q)$ for two-dimensional systems may be different from that in the one-dimensional case, since the definition of $Z_m^q(l)$ depends on the dimensionality of the system [In the one-dimensional case,[11] we defined the difference field as $Z(x):=|dX(x)/dx|$. In that case, the PDFs (probability distribution functions) of the measure $m(x;l)$ roughly collapse under rescaling. With the definition given in Eq. (14), this does not hold in two dimensions, as we see in Sec. VII.], while $Z_h^q(l)$ is always defined along a line.

Let us proceed to the numerical results. The coupling strength K is fixed at 0.85 hereafter, where the system is fully in the anomalous spatio-temporal chaotic regime.

Figure 9 displays the partition function $Z_h^q(l)$ obtained for several values of q. Each curve depends on l in a power-law manner for small l, and the corresponding exponent increases with q. The dependence of the scaling exponent $\zeta(q)$ on q is shown in Fig. 10. The $\zeta(q)$ curve is a strongly nonlinear function of q, and the multiscaling property of the amplitude field is evident. Furthermore, the $\zeta(q)$ curve possesses a bi-linear form, as expected from Eq. (19), although a sharp transition is absent, due to the limited number of oscillators [There exists another asymptotic regime near the transition point, where $Z_h^q(l)$ does not behave in a power-law manner.[6,7] The measured exponents deviate from the theoretical values in this regime. With an increase in N, this asymptotic regime shrinks, and the transition becomes clearer (see inset of Fig. 10).]. From the large q behavior of the exponent, we can roughly estimate the value of β as ~ 0.45.

Thus, the amplitude field turns out to be multiaffine, and the behavior of the scaling exponent is the same as that in the one-dimensional case.

Figure 11 shows the partition function $Z_m^q(l)$ for several values of q. It is clear that each curve exhibits a power-law dependence on l. The width of the region in which the power law holds seems much wider than in the previous case. The scaling exponent $\tau(q)$ is plotted in Fig. 12. The corresponding generalized dimension $D(q):=\tau(q)/(q-1)$ is also shown in the inset. $\tau(q)$ is again a nonlinear function of q, but its dependence on q does not seem to be so simple as that

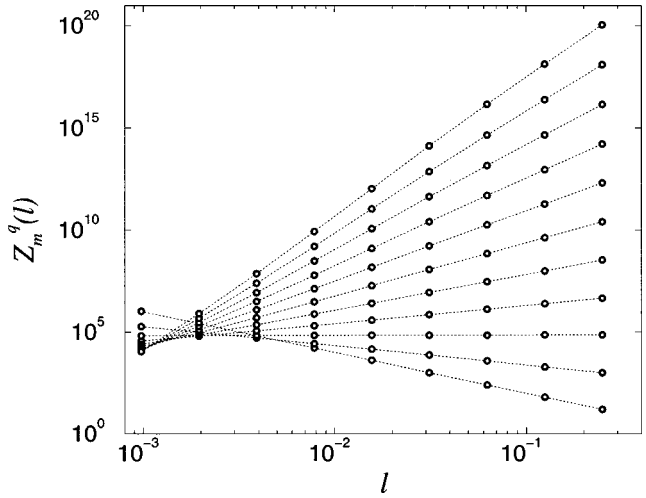

FIG. 11. Partition functions $Z_m^q(l)$ for several values of q, at intervals of 0.5. The bottom line corresponds to $q=0$ and the top one to $q=5$.

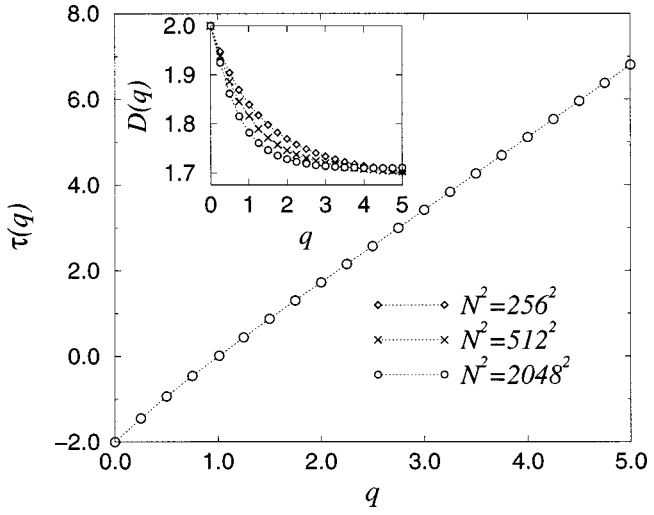

FIG. 12. Scaling exponent $\tau(q)$ obtained for $N^2=2048^2$. The inset shows the corresponding generalized dimension $D(q)$ for the cases $N^2=256^2$, 512^2, and 2048^2.

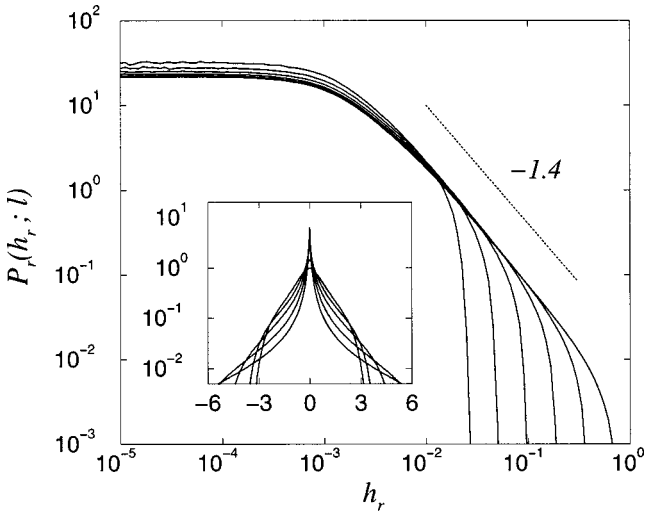

FIG. 13. Rescaled PDFs $P_r(h_r;l)$ for $l=\sqrt{2}$, $2\sqrt{2}$, $4\sqrt{2}$, $8\sqrt{2}$, $16\sqrt{2}$, and $32\sqrt{2}$ ($\times 1024^{-1}$). The curve with the slowest cutoff corresponds to $l=\sqrt{2}\times 1024^{-1}$, and the leftmost curve with the fastest cutoff corresponds to $l=32\sqrt{2}\times 1024^{-1}$. The inset shows the PDFs of the amplitude difference $h(l)$ (without taking the absolute value), rescaled by the standard deviation on a log-linear scale for $l=\sqrt{2}$ (the steepest curve), $4\sqrt{2}$, $16\sqrt{2}$, $64\sqrt{2}$, and $128\sqrt{2}$ (the nearly quadratic curve) ($\times 1024^{-1}$).

of $\zeta(q)$. However, as we conjectured (based on the results of our numerical analysis) in the one-dimensional case,[11] $\tau(q)$ seems to depend linearly on q in the asymptotic regime. Correspondingly, the $D(q)$ curve seems to saturate to a horizontal line $D(q)=D(\infty)$, and this transition becomes sharper as we increase the system size [We cannot observe a clear transition to a horizontal line, as in the one-dimensional case. This may be due to the limited number of oscillators used (We typically needed $N=2^{15}$ oscillators to observe a clear transition in one dimension. Since in two dimensions this requires $N^2=2^{30}$ oscillators, such was not possible in our present simulations.), or to the two-dimensionality of the system.].

Thus, the difference field also turns out to be multifractal. Despite the above-mentioned two-dimensionality of the system, the behavior of the scaling exponent is roughly the same as that in the one-dimensional case. In particular, it exhibits linear dependence on q asymptotically.

VII. PROBABILITY DISTRIBUTIONS OF THE MEASURES

The multiscaling properties of the amplitude and difference fields are consequences of the intermittency underlying the system. In order to analyze this intermittency in more detail, we study here the probability distribution functions (PDF) of both measures at each length scale.

Let us consider the PDFs of the measures $h(l)$ and $m(l)$. It is convenient to use the rescaled measures $h_r(l):=h(l)/l$ and $m_r(l):=m(l)/l^2$ and the corresponding rescaled PDFs $P_r(h_r;l)$ and $Q_r(m_r;l)$. With this rescaling, the peaks and widths of the PDFs become relatively close. We give our results in these rescaled variables.

The scaling exponents $\zeta(q)$ and $\tau(q)$ are fully determined by the dependence of these PDFs on the scale l. In Ref. 11, we approximated the tails of the PDFs with certain functional forms and extracted the scaling exponents asymptotically in the small l limit. Here we only present some of the numerical results for the purpose of emphasizing the intermittency of the amplitude and difference fields.

Figure 13 displays the rescaled PDF $P_r(h_r;l)$ of the rescaled amplitude difference $h_r(l)$ for several values of l on a log–log scale. Each PDF has a characteristic shape similar to the truncated Lévy distribution, as we obtained previously for the one-dimensional case. This is composed of a constant region near the origin, a power-law decay in the middle, and a sharp cutoff. Each curve roughly collapses to a scale-invariant curve in the constant and power-law regions, while the cut-off of the tail moves to the right as l decreases, due to the intermittency. More precisely, the cut-off position of the PDF (defined in some suitable way) is proportional to l^{-1}. This gives rise to the bi-fractal behavior of the $\zeta(q)$ curve (see Ref. 11 for details).

Our previous theory predicts that the slope of the power-law decay is $-1-\beta$, with the constant β from Eq. (19). This is confirmed in Fig. 13, where the slope of the power-law decay can be read off as -1.4, roughly in agreement with the previously obtained value $\beta\sim 0.45$ from the scaling exponent $\zeta(q)$. The inset of Fig. 13 displays the PDF of the amplitude difference $h(l)$ (without taking the absolute value), rescaled by the standard deviation on a linear-log scale, in order to further emphasize the intermittency of the amplitude field. The PDF evolves from a nearly Gaussian form into an intermittent power-law form as the scale l decreases.

Figure 14 displays the PDFs $Q_r(m_r;l)$ for the rescaled volume $m_r(l)$. Their shapes are not as simple as those for $P_r(h_r;l)$. They are also qualitatively different from the PDF for the difference field in the one-dimensional case[11] [The main differences are (i) the PDFs do not collapse under the rescaling, and (ii) the exponent of the power-law decay varies gradually with l. These are primarily due to the different

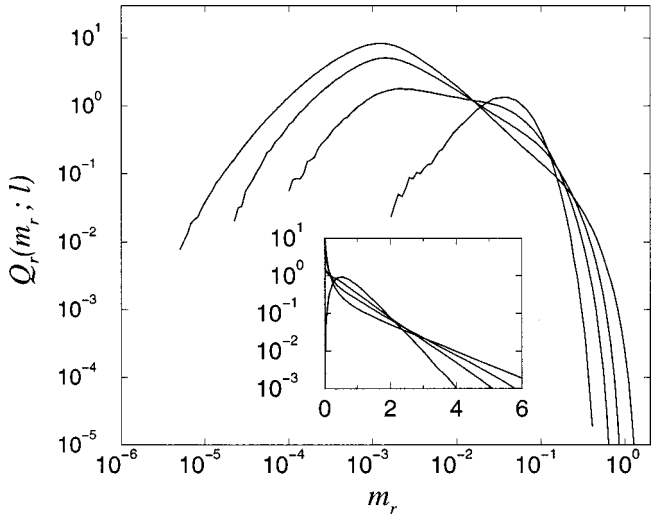

FIG. 14. Rescaled PDFs $Q_r(m_r;l)$ for $l=2$ (the widest distribution with the steepest power-law decay), 8, 32, and 128 (the narrowest) ($\times 1024^{-1}$). The inset shows the PDFs of $m(l)$, rescaled by the standard deviation on a log-linear scale for the same set of values of l. The steepest curve corresponds to $l=2\times 1024^{-1}$, and the curve with the nearly quadratic peak corresponds to $l=128\times 1024^{-1}$.

definition of the difference field $Z(\boldsymbol{r})$ from the one-dimensional case.]. However, we can still see in the present case that both tails extend, and the distribution widens as the scale l decreases. That is, as we decrease the observation scale l, largely deviated events appear more frequently. It is obvious that this intermittency effect gives rise to the nonlinearity of the scaling exponent $\tau(q)$, although the precise functional form is difficult to obtain. The inset shows the PDF of the measure $m(l)$ rescaled by the standard deviation on a linear-log scale for several values of l. The PDF gradually becomes steeper as l decreases due to the intermittency.

Hence, the PDFs of the measures reveal the intermittency of our system clearly. In particular, the PDF for the amplitude difference $h(l)$ has the same shape as that already obtained in the one-dimensional case.

VIII. CONCLUSION

We numerically analyzed a two-dimensional system of nonlocally coupled complex Ginzburg–Landau oscillators. As in the one-dimensional case, we found an anomalous spatio-temporally chaotic regime characterized by power-law behavior of the spatial correlation function. As expected from our previous theory, the amplitude difference between neighboring elements exhibits noisy on–off intermittency, giving a microscopic dynamical origin for the power-law spatial correlations. We performed a multiscaling analysis in regime exhibiting anomalous spatio-temporal chaos and found that the amplitude and difference fields are indeed multiaffine and multifractal, indicating strong intermittency underlying the system. By studying the PDFs of the measures at each length scale, the intermittency was clearly observed in the form of scale-dependent deviations of the PDFs in their tails.

Multiscaling properties are also known to exist in phenomena such as fluid turbulence and fractal surface growth. The appearance of similar multiscaling properties in many different systems suggests some underlying common statistical law. Further study of the intermittency in our system will give more insight into understanding the multiscaling properties observed in complex dissipative systems.

ACKNOWLEDGMENTS

The author gratefully acknowledges helpful advice and continuous support from Professor Yoshiki Kuramoto and thanks Dr. Axel Rossberg and Dr. Glenn Paquette for critically reading the manuscript. He also thanks the Yukawa Institute for providing computer resources, and the JSPS Research Fellowships for Young Scientists for financial support.

[1] Y. Kuramoto, *Chemical Oscillations, Waves, and Turbulence* (Springer-Verlag, Berlin, 1984).
[2] T. Bohr, M. H. Jensen, G. Paladin, and A. Vulpiani, *Dynamical Systems Approach to Turbulence* (Cambridge University Press, Cambridge, 1998).
[3] V. Hakim and W-J. Rappel, Phys. Rev. A **46**, 7347 (1992); N. Nakagawa and Y. Kuramoto, Prog. Theor. Phys. **89**, 313 (1993).
[4] K. Kaneko, Physica D **41**, 137 (1990); T. Shibata and K. Kaneko, Phys. Rev. Lett. **81**, 4116 (1998).
[5] Y. Kuramoto, Prog. Theor. Phys. **94**, 321 (1995).
[6] Y. Kuramoto and H. Nakao, Phys. Rev. Lett. **76**, 4352 (1996); **78**, 4039 (1997).
[7] H. Nakao, Phys. Rev. E **58**, 1591 (1998).
[8] A. S. Pikovsky, Phys. Lett. A **165**, 33 (1992).
[9] N. Platt, S. M. Hammel, and J. F. Heagy, Phys. Rev. Lett. **72**, 3498 (1994).
[10] A. Čenys and H. Lustfeld, J. Phys. A **29**, 11 (1996); A. Čenys, A. N. Anagnostopoulos, and G. L. Bleris, Phys. Lett. A **224**, 346 (1997).
[11] H. Nakao and Y. Kuramoto, Eur. Phys. J. B. (to be published).
[12] U. Frisch, *Turbulence—The Legacy of A. N. Kolmogorov* (Cambridge University Press, Cambridge, 1995).
[13] P. Meakin, *Fractals, scaling, and growth far from equilibrium* (Cambridge University Press, Cambridge, 1998).
[14] V. Carbone, N. Scaramuzza, and C. Versace, Physica D **106**, 314 (1997).
[15] N. Vandewalle and M. Ausloos, Eur. Phys. J. B **4**, 257 (1998).
[16] A. Turiel, G. Mato, N. Parga, and J-P. Nadal, Phys. Rev. Lett. **80**, 1098 (1998).